

Xiaochu Lou,^a Rui Bao,^a
 Cong-Zhao Zhou^b and
 Yuxing Chen^{a,b,*}

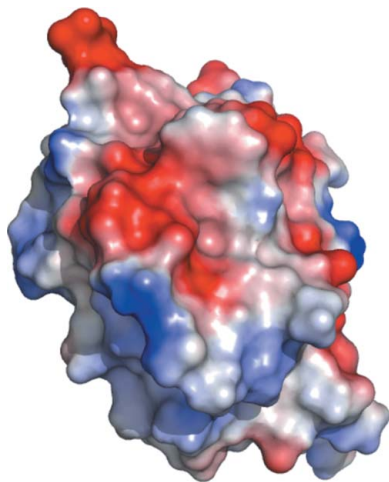
^aInstitute of Protein Research, Tongji University, Shanghai 200092, People's Republic of China, and ^bHefei National Laboratory for Physical Sciences at Microscale and School of Life Sciences, University of Science and Technology of China, Hefei, Anhui 230027, People's Republic of China

Correspondence e-mail: cyxing@ustc.edu.cn

Received 21 October 2008

Accepted 11 November 2008

PDB Reference: thioredoxin-fold domain of human phosducin-like protein 2, 3evi, r3evisf.



© 2009 International Union of Crystallography
 All rights reserved

Structure of the thioredoxin-fold domain of human phosducin-like protein 2

Human phosducin-like protein 2 (hPDCL2) has been identified as belonging to subgroup II of the phosducin (Pdc) family. The members of this family share an N-terminal helix domain and a C-terminal thioredoxin-fold (Trx-fold) domain. The X-ray crystal structure of the Trx-fold domain of hPDCL2 was solved at 2.70 Å resolution and resembled the Trx-fold domain of rat phosducin. Comparative structural analysis revealed the structural basis of their putative functional divergence.

1. Introduction

The thioredoxin-fold (Trx-fold) protein-structure classification (SCOP; <http://scop.mrc-lmb.cam.ac.uk>; Murzin *et al.*, 1995) was characterized based on the structure of *Escherichia coli* Trx1 (Holmgren *et al.*, 1975). The classic Trx fold consists of a single domain with a central five-stranded mixed β -sheet flanked by two α -helices on each side. The secondary-structure elements are arranged in the order $\beta\alpha\beta\alpha$, with β_4 antiparallel to the other strands. A set of protein families containing this fold have been identified in SCOP, including Trx, glutaredoxin (Grx; Sun *et al.*, 1998), protein disulfide isomerase (PDI; Tian *et al.*, 2006), glutaredoxin S-transferase (Reinemer *et al.*, 1991), calsequestrin (Wang *et al.*, 1998) and phosducin (Pdc; Gaudet *et al.*, 1996).

Phosducin is a 28 kDa cytosolic protein which was first found in retinal extracts (Lolley *et al.*, 1977). It was originally identified as a modulator of heterotrimeric G-protein signalling in the retina (Schroder & Lohse, 1996). Subsequently, a series of Pdc-like proteins (PhLPs) were identified in vertebrates and lower eukaryotes that constitute the Pdc family (Blaauw *et al.*, 2003). The members of this family share an N-terminal helix domain and a C-terminal Trx-fold domain (Gaudet *et al.*, 1996; Stirling *et al.*, 2007) and can be divided into three subgroups (Blaauw *et al.*, 2003). Subgroup I includes Pdc and PhLP1, subgroup II contains PhLP2 and subgroup III contains PhLP3 (Blaauw *et al.*, 2003; Willardson & Howlett, 2007). The proteins of subgroup I are the best characterized. Crystal structures of the Pdc-G_t $\beta\gamma$ complex (Gaudet *et al.*, 1996, 1999; Loew *et al.*, 1998) showed that Pdc could block G-protein signalling by disrupting the interaction between G_t α and G_t $\beta\gamma$. PhLP1 contains an 11-residue sequence corresponding to the conserved G_t $\beta\gamma$ -binding motif of Pdc in the N-terminal domain (Miles *et al.*, 1993; Blaauw *et al.*, 2003), which has been reported to play a similar role in regulating other G-protein $\beta\gamma$ subunits (Loew *et al.*, 1998) and to bind and regulate chaperonin-containing Tcp1 (CCT; Martin-Benito *et al.*, 2004). Proteins in subgroup III have been identified as modulators of CCT and to play roles in actin and tubulin biogenesis in yeast (McLaughlin *et al.*, 2002) and microtubule function in *Caenorhabditis elegans* (Stirling *et al.*, 2007). Proteins in subgroup II were reported to be essential in *Dictyostelium discoideum* and yeast (Blaauw *et al.*, 2003; Stirling *et al.*, 2007). Moreover, recent findings have indicated that most members of the Pdc family act as cochaperones with CCT (Willardson & Howlett, 2007).

In humans, five family members, hPdc, hPhLP1, hPDCL2, hPDCL3 and hPhLP3, have been recognized to date. We determined the crystal structure of the Trx-fold domain of hPDCL2, a member of subgroup II, at 2.70 Å resolution. To date, its detailed function has not been characterized.

2. Materials and methods

2.1. Cloning and protein expression

The gene encoding the Trx-fold domain (residues 88–209) of hPDCL2 (*hPDCL2*; GenBank Accession No. BC034431) was amplified by PCR from the human cDNA library (Proteintech Group Inc.). The amplified DNA was cloned into a pET29a-derived expression vector between *NcoI* and *NotI* restriction sites, which were incorporated into the sequences of the sense and antisense primers 5'-**GCCCCATGGCAAATTTGGAGAATTAAG**-3' and 5'-**GCCGCGCCGCTTAGTTTTCTTCCAAATC**-3', respectively (shown in bold). The resulting construct was verified by sequencing and contained an MHHHHHHG tag at the N-terminus of the protein as a result of the cloning strategy. *Escherichia coli* BL21 (DE3) strain cells were transformed with this construct and cultured in 600 ml LB medium containing 10 µg ml⁻¹ kanamycin at 310 K until the OD₆₀₀ reached 0.6. Protein expression was induced by adding isopropyl β-D-1-thiogalactopyranoside (IPTG) to a final concentration of 0.2 mM for 20 h at 291 K. Cells were harvested by centrifugation at 7330g for 10 min and resuspended in cold lysis buffer (20 mM Tris–HCl pH 8.0, 50 mM NaCl). The suspension was sonicated and clarified by centrifugation at 29 000g for 25 min at 277 K.

2.2. Protein purification

The supernatant was loaded onto 2 ml Ni–NTA affinity resin (Qiagen) pre-equilibrated with lysis buffer at 289 K. After washing with 20 ml lysis buffer plus 10 mM imidazole, the target protein was eluted with lysis buffer containing 250 mM imidazole and then further purified on a HiLoad 16/60 Superdex 75 column (Amersham Biosciences) equilibrated with lysis buffer at 289 K. The fractions containing the target protein were verified using SDS–PAGE.

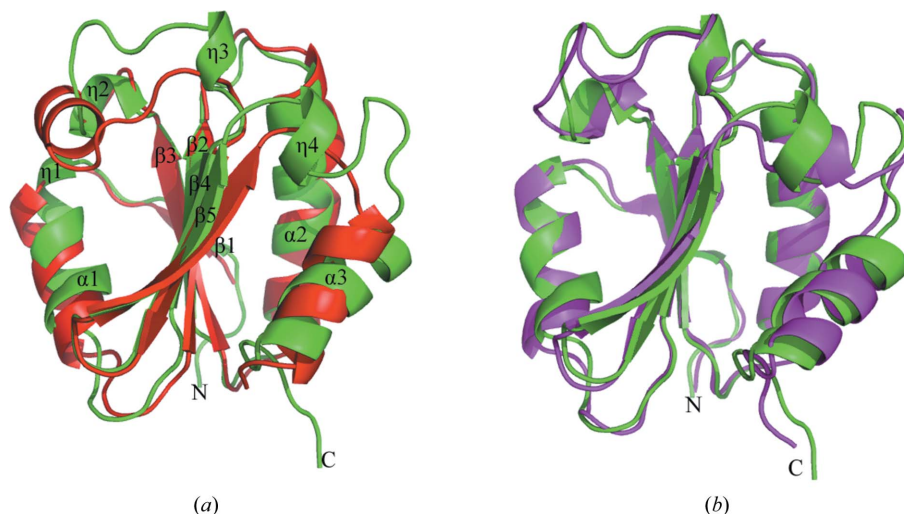


Figure 1

Overall structure superposition of the hPDCL2 Trx-fold domain (green) with (a) hTrx1 (PDB code 1aiu; red) and (b) the Trx-fold domain of rPdc (PDB code 2trc; magenta). The secondary-structure elements are labelled sequentially in (a). The figures were prepared using *Pymol* (DeLano, 2002).

Table 1

Data-collection and refinement statistics.

Values in parentheses are for the highest resolution shell.

Data collection	
Resolution range (Å)	26.14–2.70 (2.80–2.70)
Space group	<i>P</i> 3 ₁
Temperature (K)	100
Wavelength (Å)	1.5418
Unit-cell parameters	
<i>a</i> (Å)	44.59
<i>b</i> (Å)	44.59
<i>c</i> (Å)	141.97
α (°)	90.00
β (°)	90.00
γ (°)	120.00
Unique reflections	9164 (895)
Completeness (%)	93.9 (88.6)
Redundancy	2.7 (2.0)
Mean <i>I</i> /σ(<i>I</i>)	10.22 (1.53)
<i>R</i> _{merge} [†]	0.175 (0.614)
Refinement	
Resolution range (Å)	18.88–2.70
<i>R</i> _{crist} [‡]	0.236
<i>R</i> _{free} [‡]	0.276
Matthews coefficient (Å ³ Da ⁻¹)	2.79
Solvent content (%)	55.88
Mean temperature factor (Å ²)	42.30
R.m.s.d. bond lengths (Å)	0.012
R.m.s.d. bond angles (°)	1.221
Ramachandran statistics	
Residues in most favoured regions (%)	90.1
Residues in additional allowed regions (%)	9.0
Residues in generously allowed regions (%)	0.9
Residues in disallowed regions (%)	0

[†] $R_{\text{merge}} = \frac{\sum_{hkl} \sum_i |I_i(hkl) - \langle I(hkl) \rangle|}{\sum_{hkl} \sum_i I_i(hkl)}$, where $\langle I(hkl) \rangle$ is the mean intensity of *i* reflections with intensities $I_i(hkl)$ and common indices *hkl*. [‡] R_{crist} and $R_{\text{free}} = \frac{\sum_{hkl} ||F_o| - |F_c||}{\sum_{hkl} |F_o|}$; R_{free} was calculated for a 4.7% set of reflections excluded from refinement.

2.3. Crystallization and X-ray data collection

Purified protein solution (20 mM Tris–HCl pH 8.0, 50 mM NaCl) was concentrated to 8 mg ml⁻¹ by ultrafiltration (Millipore Amicon) and treated with 4 mM dithiothreitol (DTT) for 1 h. Crystallization conditions were screened by the sitting-drop vapour-diffusion method at 291 K using Crystal Screens I and II (Hampton Research). The drops consisted of 1 µl protein solution and 1 µl reservoir solu-

tion and were equilibrated against 100 μ l reservoir solution using a 48-well sitting-drop plate (XtalQuest, Beijing). After optimization, crystals suitable for X-ray diffraction grew within 3 d in a condition consisting of 28% (w/v) PEG 8000, 0.2 M ammonium sulfate. Crystals were flash-frozen in liquid nitrogen using a cryoprotectant consisting of the reservoir solution plus 25% glycerol. Diffraction data were collected to 2.70 Å resolution at 100 K using an in-house Rigaku MM007 X-ray generator ($\lambda = 1.5418$ Å) with a MAR Research 345 detector at the School of Life Sciences, University of Science and Technology of China (USTC; Hefei, People's Republic of China). The program *HKL-2000* (Otwinowski & Minor, 1997) was used for data processing and scaling and data-collection statistics are shown in Table 1. The R_{merge} value is relatively high owing to the diffraction anisotropy of the crystal. The crystal belongs to space group $P3_1$, with a Matthews coefficient of 2.79 Å³ Da⁻¹ and a solvent content of 55.88% (Matthews, 1968), suggesting the presence of two molecules in an asymmetric unit.

2.4. Structure determination and refinement

Structure solution was achieved by molecular replacement using *Phaser* from the *CCP4* suite (Collaborative Computational Project, Number 4, 1994) with the NMR structure of the Trx-like domain of mouse Pdc-like protein 2 (mPDCL2; PDB code 2dbc) as a search model. The programs *Coot* (Emsley & Cowtan, 2004) and *REFMAC5* (Murshudov *et al.*, 1997) were used to build and refine the final model, which consists of residues 88–205.

3. Result and discussion

3.1. Overall structure

The Trx-fold domain of hPDCL2 adopts a canonical Trx fold comprising a five-stranded central β -sheet flanked by seven helices (Fig. 1). The secondary-structure elements are arranged in the order $\beta\eta\alpha\beta\alpha\beta\eta\eta\beta\beta\eta\alpha$, with β_4 antiparallel to the other strands. The r.m.s.d.

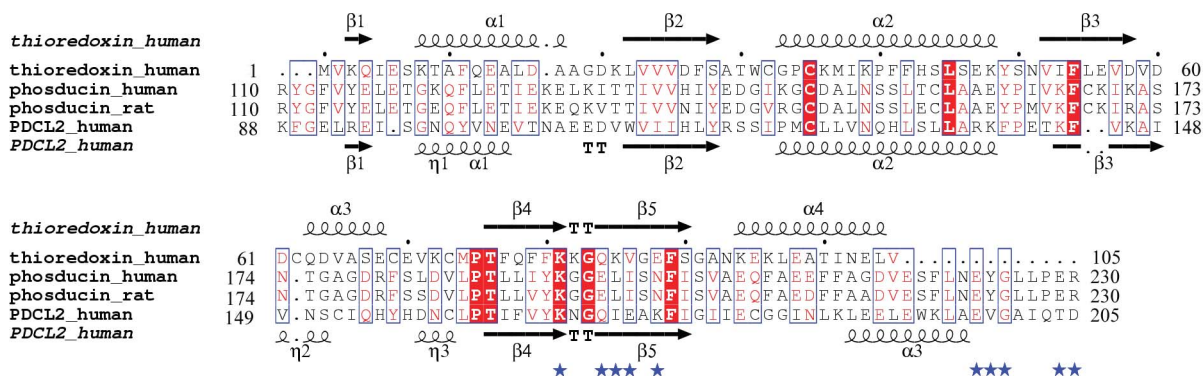


Figure 2 Structure-based sequence alignment. The sequences of hTrx1, hPdc, rPdc and hPDCL2 were obtained from the Swiss-Prot database (accession Nos. P10599, P20941, P20942 and Q8N4E4, respectively). The alignment region of each sequence is labelled at the N- and C-termini. The secondary structure of hTrx1 is shown at the top and that of the hPDCL2 Trx-fold domain is shown at the bottom. Alignments were performed using the programs *MULTALIN* (Corpet, 1988) and *ESPrpt* (Gouet *et al.*, 2003). Conserved residues are marked in red. Conserved residues in the Trx-fold domain of rPdc that contact G protein are labelled with blue stars.

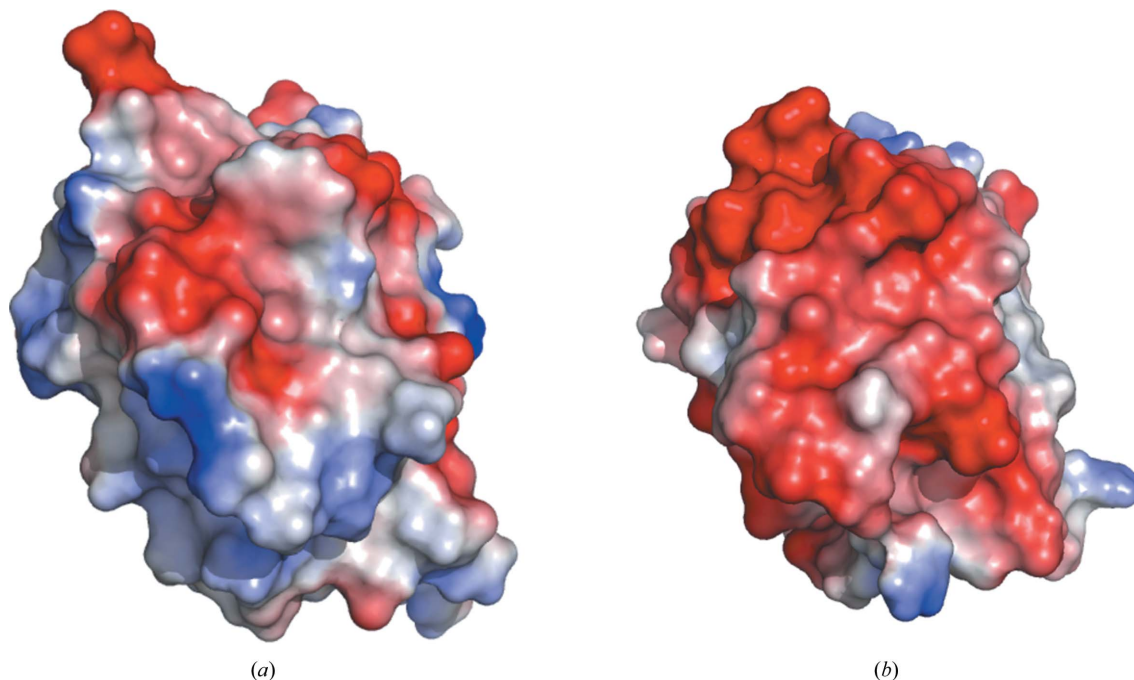


Figure 3 Electrostatic potential representations of the Trx-fold domains of (a) hPDCL2 and (b) rPdc. Figures were prepared using *PyMOL* (DeLano, 2002).

between the C^α atoms in this structure and the search model is 0.720 Å for 109 residues.

3.2. Comparison of the hPDCL2 Trx-fold domain and human Trx1

Thioredoxin is a small redox-active protein with a conserved catalytic active site (-Trp-Cys-Gly-Pro-Cys-) that undergoes reversible oxidation–reduction of two thiol groups aided by Trx reductase. The Trx-fold domain of hPDCL2 has a very low sequence homology to the classic Trx fold (19% identity and 35% similarity to human Trx1) and only contains one of the two conserved Trx active-site cysteines (Fig. 2). It can be superimposed on hTrx1 with an r.m.s. deviation (r.m.s.d.) of 1.726 Å between the C^α atoms for 87 residues and is extended compared with the classic Trx fold (Fig. 1a). Compared with the secondary-structure elements of hTrx1 (Fig. 2), helix α1 in the hPDCL2 Trx-fold domain is shorter and has an additional 3₁₀-helix η1 adjacent to its N-terminus; two 3₁₀-helices η2 and η3 with a loop between them substitute for helix α3 in hTrx1. Additionally, an extra 3₁₀-helix η4 was located between strand β5 and helix α3.

3.3. Comparison of Trx-fold domains between hPDCL2 and rPdc

The Trx-fold domain of hPDCL2 highly resembles that of rat Pdc based on a structure-homology search using the program *DALI* (Holm *et al.*, 2008). The sequence identity between the Trx-fold domains of hPDCL2 and rPdc is 24% and the corresponding r.m.s.d. between the C^α atoms is 1.194 Å for 97 residues (Figs. 1b and 2).

Although the Trx-fold domain of hPDCL2 is very similar to that of rPdc in overall structure, it contains some variations. Ten conserved residues in the rPdc Trx-fold domain were identified to bind G protein (Gaudet *et al.*, 1996). However, the Trx-fold domain of hPDCL2 only contains three of these ten conserved residues (Fig. 2), which indicates that this domain might not possess the ability to interact with G protein. Furthermore, the electrostatic potential of the hPDCL2 Trx-fold domain is greatly different from that of rPdc (Fig. 3). The Trx-fold domain of rPdc is highly negatively charged and the upper surface interacts with the β-subunit of G protein, whereas the opposite surface contributes to Gβγ translocation from the membrane (Gaudet *et al.*, 1996). The Trx-fold domain of hPDCL2 is less negatively charged than that of rPdc, especially at the surface corresponding to the membrane-interacting surface of rPdc.

In conclusion, the Trx-fold domain of hPDCL2 adopts a monothiol Trx-fold like that of rPdc in three-dimensional structure, but it lacks most of the conserved G-protein-interacting residues and exhibits a clear difference in electrostatic potential when compared with rPdc. Therefore, it could be hypothesized that hPDCL2 does not act as a modulator of G-protein signalling like rPdc.

This research was supported by projects 2006AA02A318, 2006CB910202 and 2006CB806501 from the Ministry of Science and Technology of China, grants 30470366 and 30670461 from the Chinese National Natural Science Foundation, the 100-Talent Project of the Chinese Academy of Science and a start-up fund from USTC.

References

- Blaauw, M., Knol, J. C., Kortholt, A., Roelofs, J., Ruchira, Postma, M., Visser, A. J. & van Haastert, P. J. (2003). *EMBO J.* **22**, 5047–5057.
- Collaborative Computational Project, Number 4 (1994). *Acta Cryst.* **D50**, 760–763.
- Corpet, F. (1988). *Nucleic Acids Res.* **16**, 10881–10890.
- DeLano, W. L. (2002). *The Pymol Molecular Graphics System*. <http://www.pymol.org>.
- Emsley, P. & Cowtan, K. (2004). *Acta Cryst.* **D60**, 2126–2132.
- Gaudet, R., Bohm, A. & Sigler, P. B. (1996). *Cell*, **87**, 577–588.
- Gaudet, R., Savage, J. R., McLaughlin, J. N., Willardson, B. M. & Sigler, P. B. (1999). *Mol. Cell*, **3**, 649–660.
- Gouet, P., Robert, X. & Courcelle, E. (2003). *Nucleic Acids Res.* **31**, 3320–3323.
- Holm, L., Kaariainen, S., Rosenstrom, P. & Schenkel, A. (2008). *Bioinformatics*, doi:10.1093/bioinformatics/btn507.
- Holmgren, A., Soderberg, B. O., Eklund, H. & Brändén, C. I. (1975). *Proc. Natl Acad. Sci. USA*, **72**, 2305–2309.
- Loew, A., Ho, Y. K., Blundell, T. & Bax, B. (1998). *Structure*, **6**, 1007–1019.
- Lolley, R. N., Brown, B. M. & Farber, D. B. (1977). *Biochem. Biophys. Res. Commun.* **78**, 572–578.
- Martin-Benito, J., Bertrand, S., Hu, T., Ludtke, P. J., McLaughlin, J. N., Willardson, B. M., Carrascosa, J. L. & Valpuesta, J. M. (2004). *Proc. Natl Acad. Sci. USA*, **101**, 17410–17415.
- Matthews, B. W. (1968). *J. Mol. Biol.* **33**, 491–497.
- McLaughlin, J. N., Thulin, C. D., Hart, S. J., Resing, K. A., Ahn, N. G. & Willardson, B. M. (2002). *Proc. Natl Acad. Sci. USA*, **99**, 7962–7967.
- Miles, M. F., Barhite, S., Sganga, M. & Elliott, M. (1993). *Proc. Natl Acad. Sci. USA*, **90**, 10831–10835.
- Murshudov, G. N., Vagin, A. A. & Dodson, E. J. (1997). *Acta Cryst.* **D53**, 240–255.
- Murzin, A. G., Brenner, S. E., Hubbard, T. & Chothia, C. (1995). *J. Mol. Biol.* **247**, 536–540.
- Otwinowski, Z. & Minor, W. (1997). *Methods Enzymol.* **276**, 307–326.
- Reinemer, P., Dirr, H. W., Ladenstein, R., Schaffer, J., Gallay, O. & Huber, R. (1991). *EMBO J.* **10**, 1997–2005.
- Schroder, S. & Lohse, M. J. (1996). *Proc. Natl Acad. Sci. USA*, **93**, 2100–2104.
- Stirling, P. C., Srayko, M., Takhar, K. S., Pozniakovsky, A., Hyman, A. A. & Leroux, M. R. (2007). *Mol. Biol. Cell*, **18**, 2336–2345.
- Sun, C., Berardi, M. J. & Bushweller, J. H. (1998). *J. Mol. Biol.* **280**, 687–701.
- Tian, G., Xiang, S., Noiva, R., Lennarz, W. J. & Schindelin, H. (2006). *Cell*, **124**, 61–73.
- Wang, S., Trumble, W. R., Liao, H., Wesson, C. R., Dunker, A. K. & Kang, C. H. (1998). *Nature Struct. Biol.* **5**, 476–483.
- Willardson, B. M. & Howlett, A. C. (2007). *Cell. Signal.* **19**, 2417–2427.